Journal of the Serbian Society for Computational Mechanics / Vol. 18 / No. 1, 2024 / pp 29-44 / original paper
(10.24874/jsscm.2024.18.01.03)

FIGURE OF MERIT STUDY FOR VALVELESS PIEZOELECTRIC MICROPUMP DESIGNED TO HANDLE LIQUID AND GAS FLUID IN MEDICAL AND ENVIRONMENTAL APPLICATIONS

Asma Bouzid[1,2*] [0009-0008-1147-8663], Mohamed El Amine Brixi Negassa[2] [0000-0002-1936-8599], Parastesh Pirastesh[1] [0000-0002-5078-2739], Joel Charrier[1] [0000-0001-6833-9236] and Sofiane Soulimane[2] [0009-0008-2536-9548]

[1] Institute FOTON–UMR 6082, Rennes University, Lannion, France
e-mail: asma.bouzid@univ-rennes.fr, parastesh.pirasteh-charrier@univ-rennes1.fr
[2] Biomedical department, Faculty of Technology, Tlemcen University, Tlemcen, Algeria
e-mail: mohammedelamine.brixi-nigassa@univ-tlemcen.dz
**corresponding author*

Abstract

Micropumps are revolutionizing compact and autonomous monitoring systems due to their portability and efficiency. In this paper, we present a valveless piezoelectric micropump design. This micropump distributes gas and liquid using a PDMS membrane that moves in response to a force applied by a piezoelectric actuator. The proposed design aims to achieve an average flow rate between 10 µl/min and 100 µl/min, while emphasizing mobility and low energy. For these specifications, a figure of merit (FOM) is evaluated through a parametric study of piezoelectric membrane to achieve optimized micropump performance for both gas and liquid. The finite element analysis shows the optimum thickness of PZT and PDMS, delivering a significant flow rate of 79 µl/min for liquid and 50 µl/min for gas at a lower voltage of 9 V, 60 Hz. These promising results show immense potential of micropump design in diverse applications, from intricate lab-on-a-chip platforms to precise drug delivery systems, and even integration into medical and environmental sensors.

Keywords: Micropump, piezoelectric, valveless, figure of merit (FOM), fluids, lab-on-a-chip.

1. Introduction

The advancement in Micro-Electro-Mechanical Systems (MEMS) technology has boosted the deployment of sensors in various applications (Bogue, 2007). Different sensors with several modules can be integrated on a single chip due to miniaturization, which reduces the size and the power consumption. As a result, a significant innovation has been made in many fields, particularly in key areas such as biomedical and environmental. In recent years, several scientific studies have investigated the circulation and manipulation of the fluid into sensors to develop a specific platform called a lab on a chip, drug delivery systems, and monitoring sensors. This requires the incorporation of microfluidic systems that enable precise and controllable fluid mobility at a tiny scale in these sensors. The core part of microfluidic systems is a micropump that allows for the generation of an adjustable flow rate from µl/min to ml/min (Singh et al. 2015).

Several types of micropumps based on different actuation mechanisms have been studied such as electromagnetic (Rusli et al. 2018), electrostatics (Uhlig et al. 2018), and piezoelectric (Li et al., 2021). Piezoelectric micropumps, in particular, stand out for their impressive feats: large displacements, high precision, and all this at a fraction of the energy cost (Dinh et al. 2010). This makes them ideal partners for applications such as drug delivery, lab-on-a-chip systems, and environmental monitoring. Beyond actuation, micropump design offers another choice: valve-less or valved. Valveless micropumps depend on advanced fluidic passages and dynamic interactions between fluid and microchannel architecture (Gidde et al. 2020).

Valved pumps, on the other hand, use active or passive valves to control direction and flow (Aboubakri et al., 2020), (Labdelli and Soulimane, 2020). Choosing between these two depends on the needs of the application. Valveless pumps are favored for their simplicity, compactness, and reduced risk of clogs due to the absence of moving components (Stemme and Stemme, 1993) compared with valved micropumps, which are potentially more complex but can provide finer control over fluid dynamics, making them indispensable for applications demanding precise fluid dosing, mixing, or sequential operations. So, whether it is a tiny lab-on-a-chip analyzing a single drop of blood or a miniature sensor monitoring the environment, micropumps are the powerhouses driving these innovations with their diverse actuation mechanisms and smart designs. In biomedicine, micropumps can be combined with glucose sensors to deliver continuous and controlled insulin doses for diabetics, aiding in the maintenance of stable blood sugar levels (Liu et al., 2014). This integration of biosensors and micropumps also enables the monitoring, identification, and diagnosis of various physiological and biological parameters (Ciuti et al. 2015). Real-time environmental surveillance of water and air quality becomes a reality with the integration of micropumps and optical sensors (Butt et al. 2022). This allows for the immediate detection and potential identification of contaminants and toxins in both water and air.

Micropump research has seen diverse paths, with some focusing on gas pumping (Wang et al. 2016), (Cheng et al. 2015) and others on liquids (Munas et al., 2018), (Wang et al. 2006), (Slami and Soulimane, 2022). Our work aims to develop a micropump capable of handling both gas and liquid fluids while operating at a low voltage. To achieve this, the Figure of merit (FOM) has been extracted and evaluated. This parameter represents the ratio between the piezoelectric membrane deflection and the applied voltage. Our ultimate goal is to maximize the FOM through a parametric study of thickness of lead zirconate titanate (PZT) and polydimethylsiloxane (PDMS) membranes as a function of applied voltage.

This paper is structured into four sections. The first section serves to introduce the pivotal role of micropumps in biomedicine and environmental fields and discuss the different type of micropump used to handle gas and liquid reported in the literature. Subsequently, the methodology section discusses the operational mechanics of a valveless piezoelectric micropump. It covers the modeling and simulation of a three-dimensional 3D micropump design using finite element analysis, as well as the optimization process for pumping both gas and liquid by analyzing the FOM. The results, including a comparative analysis with the existing work, are examined and discussed in the following section. Finally, the paper concludes with a final synthesis.

2. Method

2.1 Operation mechanism of the valveless piezoelectric micropump

The structure of a valveless piezoelectric micropump is depicted in Fig. 1, it consists of a pumping chamber with an oscillating membrane at the top. A piezoelectric actuator moves the membrane by applying a voltage. The alternate movement of the membrane causes volume changes within the pumping chamber, allowing continuous fluid circulation from port 1 to port 2. To control the fluid direction, a channel with a specific geometry must be incorporated at port 1 and port 2. Based on the specified shape of the canal and the fluid direction, we distinguish two channels. A widening channel in the direction of fluid flow is referred to as a "diffuser". Conversely, it is called a "nozzle" when the channel converges against the direction of fluid flow. The function of the diffuser/nozzle is to increase fluid pressure and reduce fluid velocity. This allows fluid flow regulation and precise directional control. The diffuser/nozzle also has the advantage of a simple design, which reduces the difficulty of the manufacturing and packaging processes and can operate well without external power (Nafea et al. 2019).

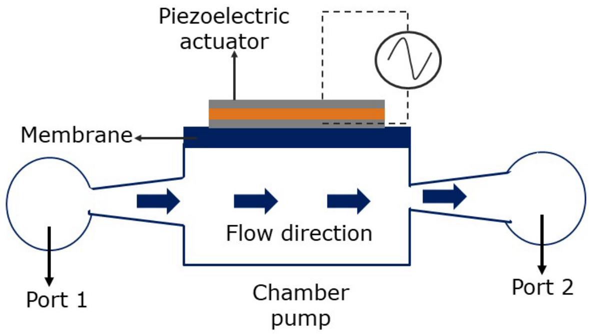

Fig. 1. Structure of a valveless piezoelectric micropump

In one vibration cycle, the oscillation movement of the piezoelectric actuator caused by applying an alternative voltage can be divided into two phases: aspiration and expiration phases. An operation mechanism schematic of a valveless piezoelectric micropump is presented in Fig. 2. In the aspiration mode (Fig. 2a), a positive voltage across the piezoelectric element forced the membrane to bend upwards, causing a higher differential pressure at port 1 than at the chamber, increasing the internal volume of the pumping chamber, and forcing the fluid to enter both port 1 and port 2. The specific shape of the diffuser/nozzle channels plays a role in regulating this fluid flow, which allows a higher flow rate to enter through the diffuser compared to backflow via the nozzle channel. Applying a negative voltage during the expiration mode (Fig. 2b) causes the membrane to move downwards. As a result, more fluid is pushed through the port 2 compared to the volume of fluid pushed through Port 1.

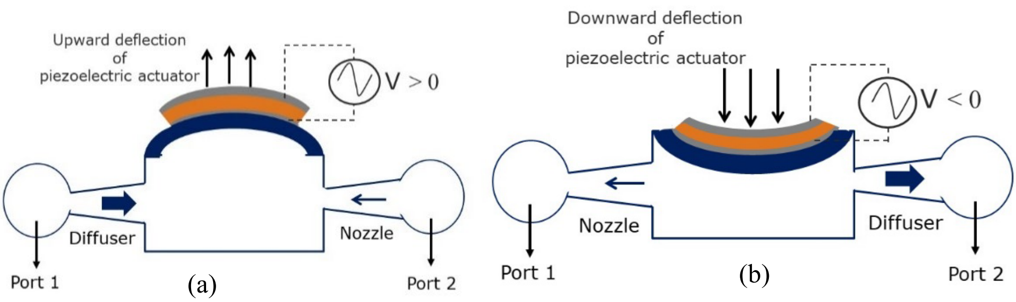

Fig. 2. Operation mechanism of a valveless piezoelectric micropump. (a) Aspiration mode; (b) Expiration mode

A net flow ($Qnet$) created over time as a result of alternating between these two phases is given by the equation (1):

$$Q_{net} = \frac{1}{2}\int_0^T Q_{port2} - Q_{port1} \tag{1}$$

Where T is the period of a pumping cycle.

The difference between the input pressure ($P_{Aspiration}$) and output pressure ($P_{Expiration}$) is the back pressure (P_{max}) and it determined by the equation (2):

$$P_{max} = P_{Expiration} - P_{Aspiration} \tag{2}$$

2.2 Modelling and simulation

2.2.1 Selected design

Finite Element Method (FEM) is used to evaluate a three-dimensional 3D design of a valveless piezoelectric micropump. The main objective is to determine the size of the micropump for potential use as an environmental sensor and in biomedical applications. To meet the requirement of portability, the micropump needed to deliver a flow rate ranging from 10 to a few hundred µl/min at the lowest possible voltage.

The design consists of two components: the actuator and the fluidic structure, as illustrated in Fig. 3. The actuator is comprised of a piezoelectric actuator attached to a thin membrane, which is fixed at the edges only (Fig. 3a). This configuration enables the membrane to move up and down. The fluidic structure comprises a circular chamber connected to two planar diffuser/nozzle elements on each side.

In this study, the dimensions of the fluidic structure are fixed, as specified in Table 1. The circular chamber has a radius (*R_chamber*) of 5 mm and a height (*H_chamber*) of 500 µm. The diffuser/nozzle elements have a length (L) of 700 µm, a wide opening (*Wo)* of 300 µm, and a small opening (*So*) of 100 µm, as illustrated in Fig. 3b. On the other hand, the thickness of the membrane (*Th_membrane*) and the thickness of the Piezo electric material (*Th_piezo*) could be varied to evaluate their impact on the FOM in order to obtain the optimum micropump design.

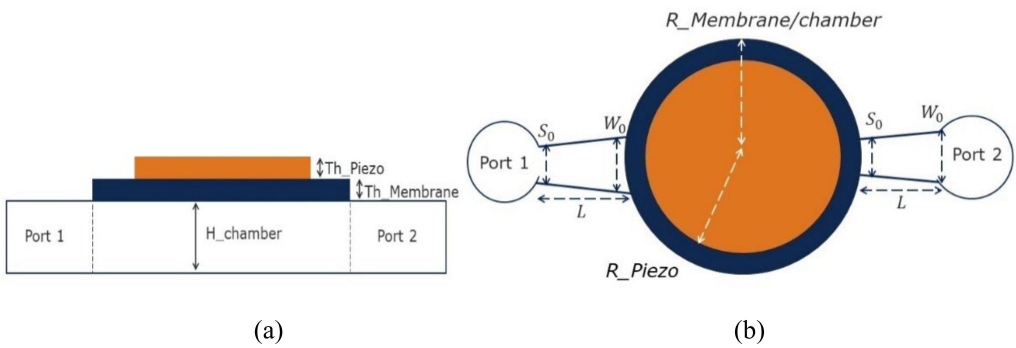

Fig. 3. Design of a valveless piezoelectric micropump for transporting gases and liquids fluid. (a) Micropump cross-section view; (b) Micropump top view.

The physical material characteristics of the micropump used in modeling are given in Table 1. PZT-5H was chosen as a piezoelectric actuator material because of its performance due to its highest piezoelectric coefficients compared to other materials. PDMS was chosen for both membrane material and fluidic structure because of its qualities: excellent durability and flexibility, as well as the fact that it is a fully biocompatible material (Sta Apolónia et al., 2019). Air and water were chosen as fluids to simulate, since air contains toxic gases and water contains emergent pollution particles in low concentrations.

Parts	Size	Material	Parameter	Value
Piezoelectric actuator	*R_Piezo* = 4.5mm *Th_piezo*= 300 µm	PZT-5H	Density Relative permittivity Piezoelectricity	7500 kg/m3 [3130, 3130, 3400] $\frac{\begin{bmatrix} 0 & 0 & 0 & 0 & 7.41e-010 & 0 \\ 0 & 0 & 0 & 7.41e-10 & 0 & 0 \\ -2.74e-10 & 2.74e-10 & 5.93e-10 & 0 & 0 & 0 \end{bmatrix} C}{N}$
Membrane	*R_membrane* = 5mm *Th_piezo*= 600 µm	PDMS	Density Young's modulus Poisson's ratio	965 Kg/m^3 750 kPa 0.49
Fluidic Structure	Chamber: *R_chamber* = 5 mm *H_Chamber*= 500 µm Diffuser/Nozzle: *L*= 700 µm *Wo* = 300 µm *So* =100 µm	Water	Density Dynamic viscosity	998.2 kg/m^3 2.414×10^{-5} Pa s
		Air	Density Dynamic viscosity	1.992 kg/m^3 1.84×10^{-5} Pa s

Table 1. Dimensions and physical material characteristics of a micropump

2.2.2 Boundary and initial conditions

The simulation is based on two physical phenomena and their interactions: piezoelectric actuation and fluidic structure. Their interaction, known as Fluid-Structure Interaction (FSI), involves the coupling of fluid flow analysis with solid mechanics analysis. Figure 4 shows the fluid-structure interaction of a valveless piezoelectric micropump.

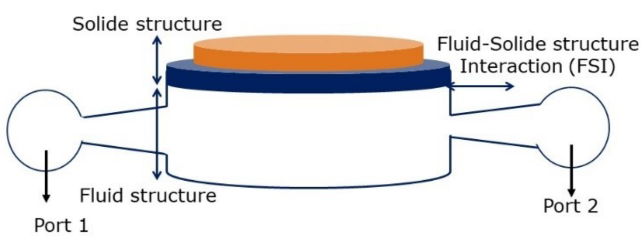

Fig. 4. Fluid-structure interaction of a valveless piezoelectric micropump

In this research, piezoelectric propriety was investigated to create an alternative deflection of membrane in both spatial and temporal dimensions when a piezoelectric material is polarized by an electric field. The equation that governs this deflection of the membrane, denoted as 'W,' is as follows (3) (Singh et al., 2015):

$$\frac{Eh^3}{12(1-\vartheta^2)}\nabla^4 W + hp_m \frac{\vartheta^2}{\vartheta t^2} = f_a - P \tag{3}$$

where E, p_m, ϑ and h are Young's modulus, density, Poisson's ratio and thickness of the membrane, respectively, and t is the time. ∇^4 is the two-dimensional double Laplacian operator, f is the periodic force (due to PZT actuator) acting in the membrane, and P is the dynamic pressure exerted by the fluid on the membrane.

The relationship between the electric field applied to the PZT actuator and the structural deflection is described by the following equations (4) and (5):

$$S_{ij} = S_{jk}^{E} T_k + d_{kj} E_k \tag{4}$$

$$D_i = d_{ij} T_j + \in_{ij}^{T} E_j \tag{5}$$

where S is the mechanical strain, S^E is the elastic compliance coefficient at constant electric field, T is the mechanical stress, d is the piezoelectric strain coefficient, D is the electric displacement, E is the electric field, $\in^T$ is the permittivity at constant stress. Additionally, we use vector notations i, j, and k to denote the directions along the x, y, and z axes, respectively.

The PZT element is actuated by applying a sinusoidal voltage expressed as $V(t) = V_0 \sin(2\pi f t)$, where V_0 represents the amplitude of the voltage, f is the frequency, and t denotes time. The initial values of voltage and frequency selected are 60 V and 60 Hz.

In this paper, the micropump was tested using two different types of fluids, namely liquid and gas. Each fluid in the micropump presents its own dynamic behavior. The following descriptions of water fluid dynamics inside the micropump are given by the incompressible Navier-Stokes equations (6) and (7), which include the continuity equation and momentum equations. It is assumed that the fluid inside the pump is laminar:

$$\rho \nabla \vec{u} = 0 \tag{6}$$

$$\rho \left(\frac{\vartheta \vec{u}}{\vartheta t} \nabla \right) \vec{u} = -\nabla P + \mu \nabla^2 \vec{u} \tag{7}$$

Nevertheless, the gas is considered a compressible fluid and the governing equations (8) and (9) are given for its movement inside the micropump:

$$\frac{\vartheta \rho}{\vartheta t} + \nabla \rho \vec{u} = 0 \tag{8}$$

$$\rho\left(\frac{\vartheta\vec{u}}{\vartheta t}\nabla\right)\vec{u} = -\nabla P + \mu\nabla^2\vec{u} \tag{9}$$

where $\vec{u}$ is the velocity vector and ρ, μ and P are the fluid density, dynamic viscosity and pressure, respectively.

Solid structure (membrane actuator) and fluid were combined by the FSI interface to explore interactions between them. This integration involves incorporating solid mechanics within the material frame using a Lagrangian description as well as describing fluid flow within the spatial frame using a Eulerian approach. This is accomplished through the application of an arbitrary Lagrangian-Eulerian (ALE) technique.

Simulation equations require proper boundary and initial conditions which are crucial for accurate system behavior over time and real-world reflection. Input criteria provide the starting point, while boundary conditions establish interactions between the system and its environment. Zero displacement limit criteria and defined fixed constraints around the PDMS membrane margins were established. Pressure boundary conditions (uniform zero pressure) were imposed at the fluid domain's ports 1 and 2 and all walls were subject to a no-slip boundary condition.

Increased mesh elements in the structure lead to longer computation times. Balancing mesh refinement for accuracy and efficiency is crucial for optimization. A finer free tetrahedral mesh was adopted for the structural simulation, allowing for more accurate geometry reproduction, and capturing finer details. Figure 5 displays the mesh used for the valveless piezoelectric micropump. To study the micropump's dynamic behavior, a time-dependent analysis is included, allowing to observe its operation and changes over time.

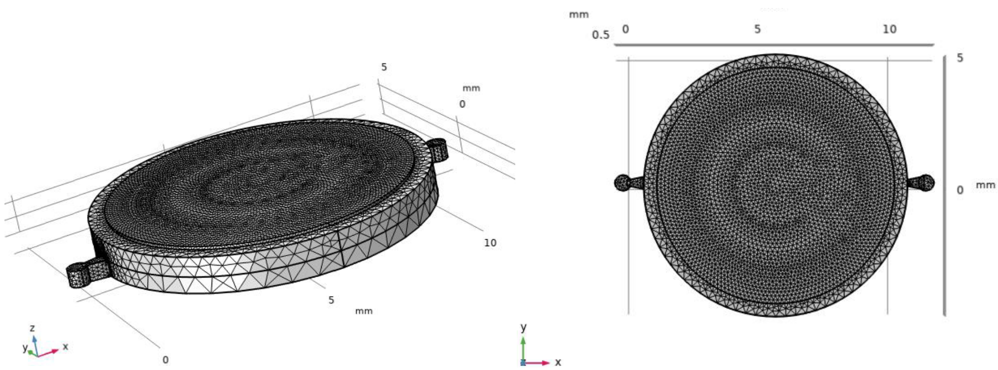

Fig. 5. Mesh of a valveless piezoelectric micropump

The simulation of water as a fluid circulating in a micropump was initiated. For this, a 300 µm thick PZT deposed on 600 µm thick PDMS was polarized by a sinusoidal voltage $V(t) = V_0 \sin(2\pi f t)$, where V_0 equal to 60 V and the frequency is 60 Hz. Figure 6 illustrates the correlation and synergism between the applied voltage and membrane displacement (deflection) and flow rate of port 1 and port 2.

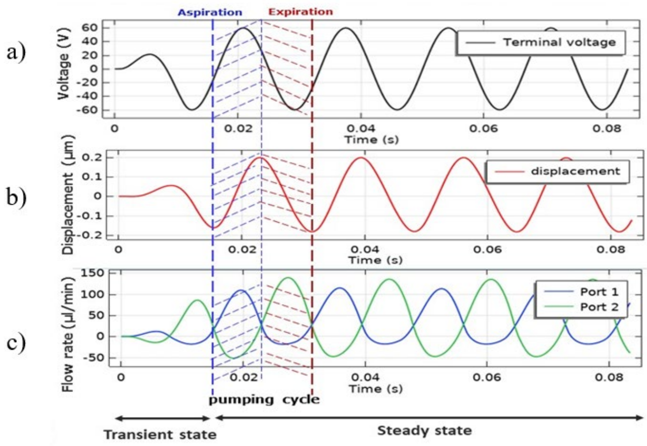

Fig. 6. a) Voltage applied to a piezoelectric actuator; b) displacement of piezoelectric membrane; c) the flow rate in the aspiration and expiration phases of water fluid

A transient state was observed at the start of pumping, followed by the stabilization of the pump rhythm. A positive voltage causes the membrane to deflect upward, sucking in the fluid through both ports 1 and 2. However, port 1 sips twice as much as port 2, revealing a preference for inspiration. Flipping the voltage polarity flips the script: forcing the membrane to bend downward, expelling the fluid with port 2 dominating, sending out 14 times more liquid than port 1. These results illustrate the behavior of the micro-pump and how the fluid circulates inside the micropump.

2. 3 Optimization the performance of a piezoelectric micropump

The integration of such a piezoelectric micropump into biomedical and environmental sensors is challenging due to the applied voltage of 60 V. Even if this voltage can produce a flow rate of up to 100 µl/min, the portability of the sensor is severely limited. Consequently, it is crucial to increase the micropump efficiency by reducing the applied voltage while maintaining an important membrane deflection to generate substantial flow rates. To achieve this, the ratio between the deflection of the membrane and the voltage applied is described in the FOM and it is evaluated by membrane piezoelectric parametric studies to optimize the design and performance of the micropump for both gas and liquid fluid. The objective is to obtain a higher FOM by reducing the voltage (V) and increasing the membrane deflection (D), which increases the flow of micropump. The equation (10) defines the FOM:

$$FOM = \frac{D}{V}(\mu m / V) \tag{10}$$

3. Results and discussion

3. 1 Water simulation

The performance of the microfluidic system proposed for both gas and liquids was investigated through simulations, initially focusing on water, applying voltage from 1.5 V to 30 V, and varying PZT thickness from 100 µm to 500 µm (with a fixed PDMS thickness of 600 µm). The FOM was analyzed to understand the impact of voltage on the membrane deflection and flow rate. Figure 7 shows the FOM evolution, inflow and outflow as a function of PZT thickness and voltage for the water fluid.

The results depicted in Fig. 7a show a constant FOM for each PZT thickness at different voltages, indicating a linear deflection-voltage relationship. Thinner PZT layers yielded higher FOMs, with a maximum of 0.013 µm/V achieved at 100 µm. Deflection increased from 120 nm at 9 V to 280 nm at 30 V. Both inflow and outflow rates rose with voltage and decreased with PZT thickness, reaching a maximum of 270 µl/min and 252 µl/min for the inflow and outflow (Fig 7. a, b), respectively, at 30 V and 100 µm PZT thickness. This confirms a reciprocal relationship between the flow rate, voltage, and deflection, which is justified by the fact that the PZT thickness is finer, i.e. it has less rigidity, which leads to great displacement, which in turn generates a higher flow rate.

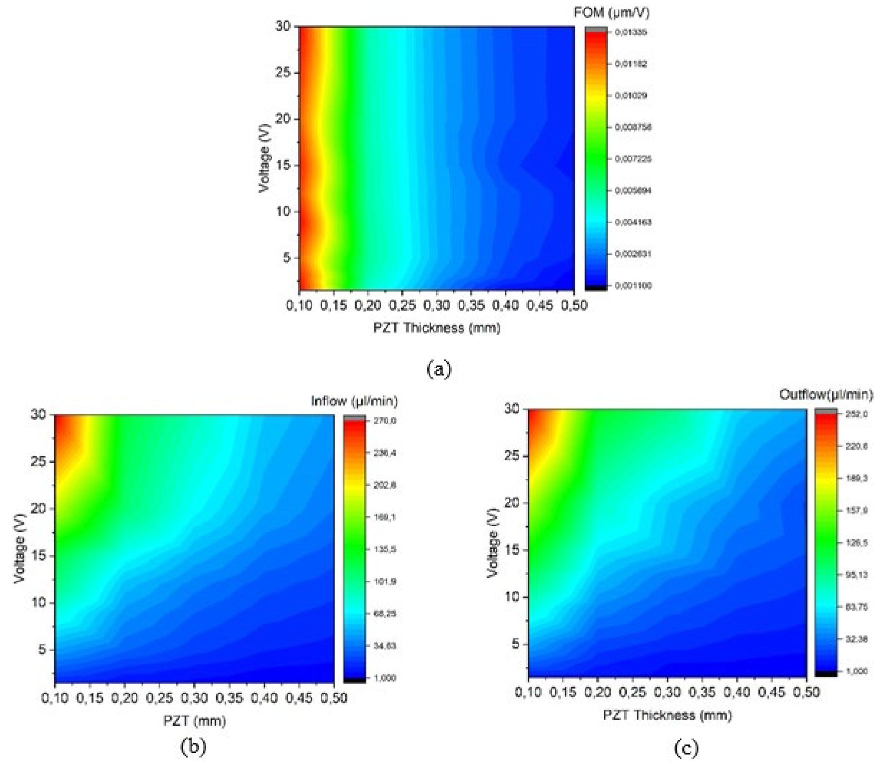

Fig. 7. a) Figure of merit (FOM); b) inflow; (c) outflow, as a function of the PZT with a fixed 0.6 mm for water fluid

In order to achieve an optimum FOM and obtain an important flow rate, a PDMS membrane thickness is analyzed. For this study, the thickness of both PDMS and PZT was varied from 100 µm to 1 mm and from 100 µm to 500 µm, respectively. The piezoelectric actuator was polarized by a sinusoidal voltage in the range of 1.5 V to 30 V. The results illustrated in Fig. 8 demonstrate that the FOM increases as PDMS thickness increases and decreases as PZT thickness rises. It reached the maximum between 400 µm to 600 µm of PDMS thickness. This interval of PDMS thickness led to an optimum balance between the sufficient rigidity to hold the membrane in place and the flexibility to allow maximum deflection. As the thickness of the PDMS increases, the rigidity of the membrane increases, and as a result, the deflection of the membrane decreases.

Additionally, a maximum FOM of 0.014 µm/V is obtained at 600 µm PDMS and 100 µm PZT thickness, corresponding to a constant ratio between 120 nm of deflection and 9 V of the voltage applied, which drive an inflow and outflow rate of 100 µl/min. At a thinner PDMS membrane from 100 µm to 200 µm, we observed a flow rate that ranged from 5 µl/min to 70 µl/min. However, its handling and fabrication are difficult, and there might be reliability challenges.

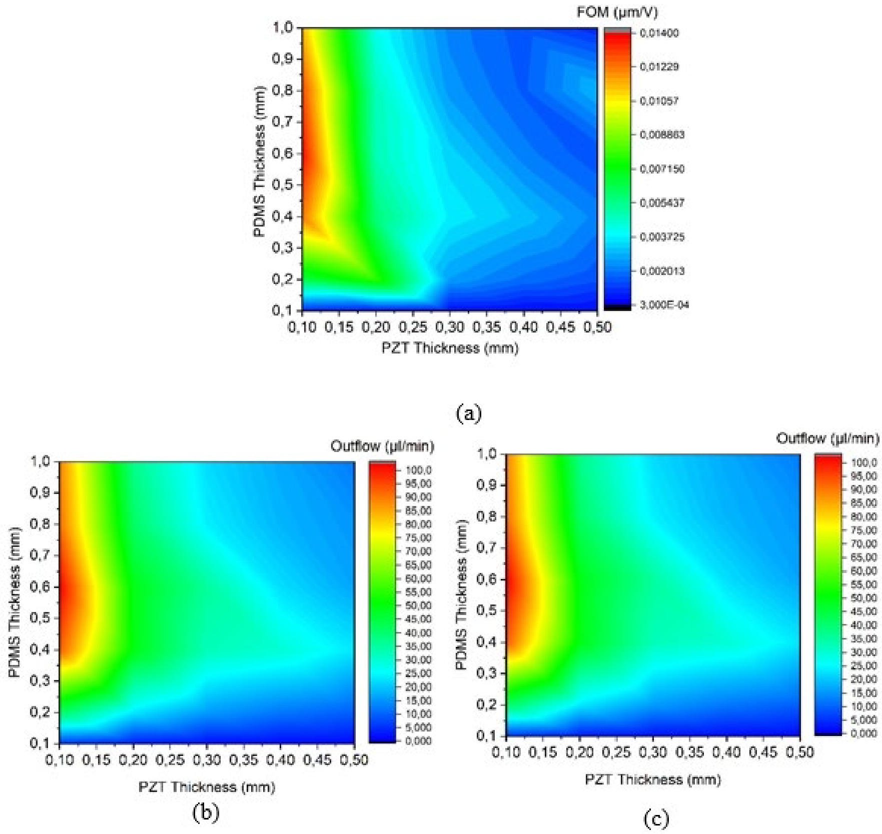

Fig. 8. a) Figure of merit (FOM); b) inflow; (c) outflow, as a function of the PZT and PDMS thickness for water fluid

3.2 Gas simulation

After simulating a micropump using water liquid, the efficiency of the micropump in handling gas was examined, and the flow rate pumped was quantified by evaluating the FOM. Air was selected as a representative gas for real time monitoring because it contains several toxic gases, including CO2, that are typically found in low concentrations in the atmosphere. Figure 9 shows the FOM, inflow, and outflow as a function of PZT thickness and voltage for air fluid, fixing PDMS thickness at 600 µm. The results demonstrate that 0.0085 µm/V is the higher FOM obtained at 100 µm PZT thickness. The large deflection of the membrane is achieved by the excellent flexibility of the 100 µm thick PZT, which generates a significant inflow and outflow, reaching a maximum of 160 µl/min and 180 µl/min, respectively, at 30 V. At a low voltage ranging from 1.5 V to 9 V, the inflow and outflow from 41 µl/min to 45.75 µl/min are reached. More than 100 µl/min is obtained by increasing the voltage applied.

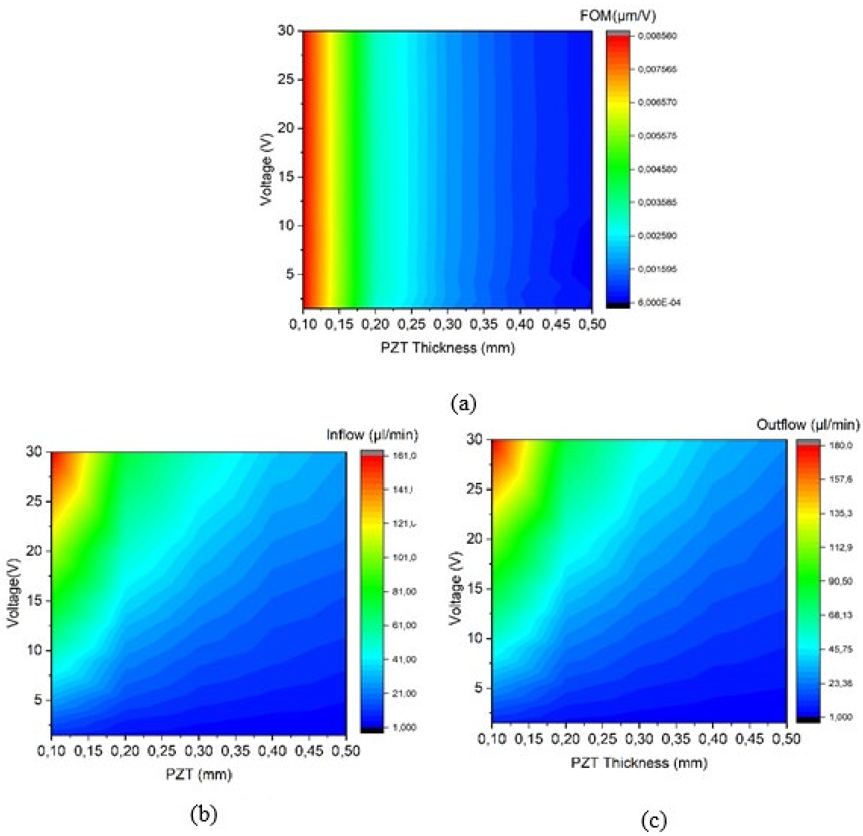

Fig. 9. a) Figure of merit (FOM); b) inflow; (c) outflow as a function of the PZT thickness and voltage with a fixed 0.6 mm PDMS thickness for gas fluid

As we examined the impact of PDMS thickness on membrane displacement under various polarization voltages, the study for gas was replicated. The FOM, inflow, and outflow results are illustrated in Fig. 10. Applying voltage in the range from 1.5 V to 30 V leads to a higher FOM at thinner PZT and PDMS thickness. At 100 µm PZT thickness deposed under 100 µm and 200 µm of PDMS, we observed a constant FOM that was equal to 0.01 µm/V. Starting by applying low voltage ranging from 1.5 V to 5 V, the deflection of the membrane increased from 30 nm to 93 nm, which led to an increase in the flow pumped via port 2 from 10.07 µl/min to 38.5 µl/min. At 9 V, the flow rate increased to 67.8 µl/min, pumped by 95 nm of membrane deflection. This last one increased from 128 nm to 322 nm at high voltages ranging from 12 V to 30 V, the flow rate started increasing from 92.1 µl/min to 234 µl/min. Thinner PDMS layers of less than 300 µm offered greater flexibility and less resistance to deformation, allowing the piezoelectric membrane to move more smoothly, resulting in a higher pumped flow rate. Compared between 600 µm and 100 µm of PDMS thickness, the 100 µm gave a higher deflection, which pumped a higher flow rate. However, there are challenges and potential quality problems in manufacturing a membrane thinner than 200 µm.

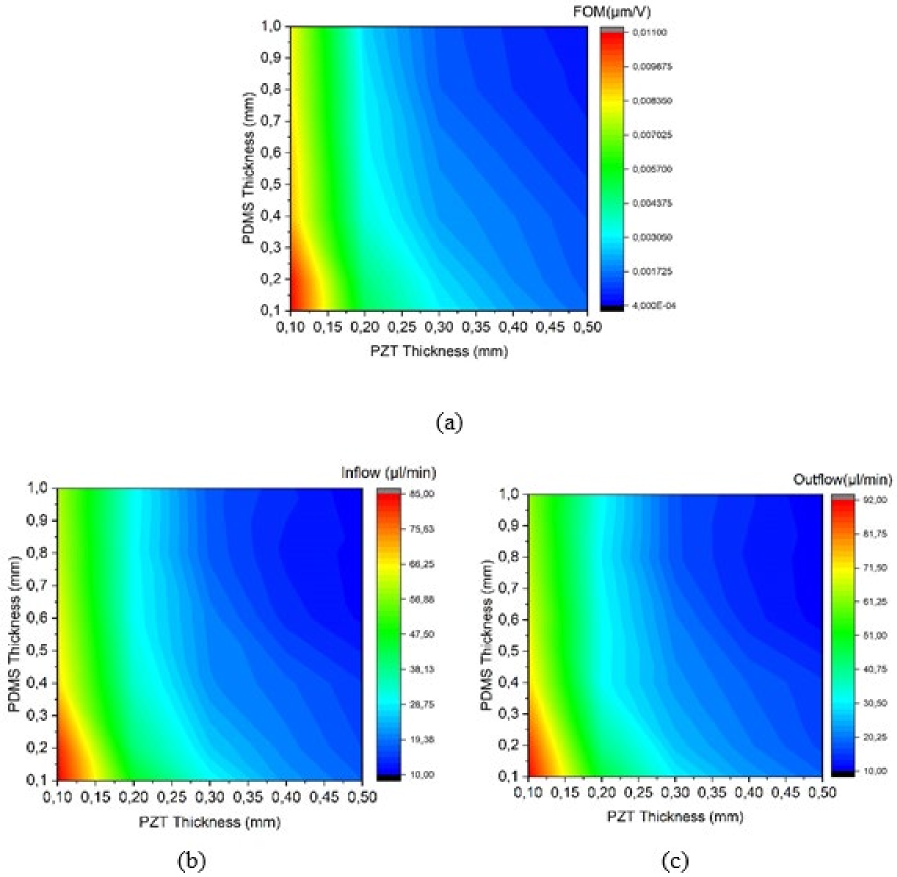

Fig. 10. a) Figure of merit (FOM); b) inflow; (c) outflow as a function of the PZT and PDMS thickness for gas fluid

3.3 Comparison of the performance of a micropump in pumping gas and liquid

Our simulations reveal crucial differences in how the valveless piezoelectric micropump handles liquids and gases. While thinner PZT layers and higher voltage boost the FOM for both, an optimal PZT thickness of 100 µm emerges for both fluids. Interestingly, PDMS thickness plays the opposing roles: increasing it makes the flow rates are higher in liquids (maximum at 600 µm), while decreasing it makes the flow rates higher in gases (maximum at 100-300 µm).

Water excels in our pump compared to gas due to its lower compressibility. Strong intermolecular forces in liquids resist pressure changes, unlike loosely packed gas molecules that easily compress (Hauptband, 2018). Remarkably, the desired flow rate range (10 µl/min to 100 µl/min) at low voltage for both liquids and gases was achieved in these simulations, validating the design goals. This paves the way for a versatile micropump that balances fluid compatibility with low power consumption, opening doors to exciting applications across various fields.

3.4 Comparison between the results obtained and state of the art

Researchers constantly strive to create an ideal micropump, each tailoring their design to specific needs. Some prioritize pumping large volumes of liquids, while others focus on efficient gas handling. Our latest design and its comparison to existing solutions were presented in Table 2. Ni et al. (2023) developed a valveless micropump able to pump 135 ml/min of air. This flow rate is achieved by higher FOM equal to 0.735 µm/V corresponding to 29.4 µm of piezoelectric actuator deflection at 40 V and 23.6 KHz. However, Singh et al. (2015) designed a circular micropump with a small size and a capacity to handle 20 µl/min of water at 200 Hz. The FOM for this micropump is 0.08 µm/V which corresponds to 2.5 µm of deflection and 30 V of polarization. Compared to the micropump built by Schabmueller et al. (2002), which is capable of controlling a flow rate for both liquid and gas, it is partially larger than the other micropumps and operates at high voltages of 190 V and 300 V under high frequencies of 2.5 KHz to 3.5 KHz It is able to generate a deflection of 5 µm that can pump a flow rate of 1500 µl/min for liquid and 690 µl/min for gas. For insulin delivery, Kaçar et al. (2020) were constructing a large circular micropump that can deliver 220 µl/min generated by 2.4 µm of piezoelectric membrane deflection at 100 V and 100 Hz. The FOM obtained is 0.024 µm/V. 0.1 µm/V of FOM generated by a small micropump that was designed by Calderon and Reyes-Betanzo (2023) to transport a lacrimal for people suffering from dry eye can deliver 1.15 µl/min when using 3 micropumps in parallel at a frequency of 1.1 KHz and 20 V.

While current pumps offer impressive features, they often come with trade-offs such as high-power consumption, large size, or limited functionality. The design proposed in this study takes a unique approach, striking a balance between performance and efficiency. At low voltage and frequency (9 V, 60 Hz), it achieves substantial flow rates (50 µl/min for gases, 79 µl/min for liquids) with a smaller FOM compared to its high-power counterparts. This translates to a compact, energy-efficient pump capable of handling both liquids and gases, making it ideal for diverse applications such as environmental sensors, lab-on-a-chip systems, and even drug delivery. This micropump represents a significant step towards high performance without compromising power consumption, opening doors to exciting advancements in microfluidic technologies.

Reference	Micropump	Size (mm)	Voltage (V)	Deflection (µm)	Frequency (Hz)	FOM (µm/V)	Flow rate (µl/min)
(Ni et al., 2023)	Gas (air)	16×16 × 5 Circular	40	29.4	23642	0.735	135000
(Schabmueller et al., 2002)	Liquid (water)	12×12× 0.85 Rectangular	190	5	2500	0.026	1500
	Gas (air)	12 ×12×0.018 Rectangular	300		3500		690
(Singh et al., 2015)	Liquid (water)	7×7×0.2 Circular	30	2.5	200	0.08	20
(Kaçar et al., 2020)	Liquid (insulin)	13.5×13 ×0.5 Circular	100	2.4	100	0.024	220
(Calderon and Reyes-Betanzo, 2023)	Liquid (synthetic lacrimal)	1.5×1.5 ×0.2 Circular	20	2	1100	0.1	0.39 and 1.15 for 3 parallel micropumps
Our work	Liquid	5×5× 0.5 Circular	9	0.12	60	0.013	79
	Gas	5×5× 0.5 Circular	9	0.0769	60	0.0085	50

Table 2. Comparison between our work and state of the art

4. Conclusions

This study unveils a valveless micropump powered by a piezoelectric actuator, designed and optimized through a finite element analysis to achieve impressive flow rates (10 µl/min to 100 µl/min) with minimal voltage for biomedical and environmental applications. The figure of merit analysis reveals key insights: higher voltage translates to greater membrane deflection for both liquids and gases, while efficiency (FOM) favors thinner PZT and thicker PDMS layers. A 100 µm PZT thickness provides optimal deflection for both fluids, with 600 µm and 100 µm PDMS thicknesses excelling in liquid and gas pumping, respectively. Even at a whisper-quiet 9 V and 60 Hz, the pump delivers substantial flow rates (79 µl/min for liquid, 50 µl/min for gas). As voltage increases, flow rates flex their muscles, reaching peaks of 252 µl/min and 234 µl/min for liquid and gas, respectively, at 30 V. These results position our micropump as a game-changer, offering precise and efficient fluid control for diverse applications: from miniature lab-on-a chip manipulations to seamlessly integrated environmental and biomedical sensors, and even controlled drug delivery with minimal energy consumption. This innovative micropump stands poised to revolutionize fluid control, opening doors to exciting advancements in various fields.

Acknowledgements: This paper was supported by the project Hubert Curien Partnerships (PHC) under 07MAG21 project.

References:

Aboubakri, A., Ahmadi, V.E., Koşar, A.,(2020). Modeling of a Passive-Valve Piezoelectric Micro-Pump: A Parametric Study. *Micromachines* 11, 752. https://doi.org/10.3390/mi11080752

Bogue, R., (2007). MEMS sensors: past, present and future. *Sens. Rev*. 27, 7–13. https://doi.org/10.1108/02602280710729068

Butt, M.A., Voronkov, G.S., Grakhova, E.P., Kutluyarov, R.V., Kazanskiy, N.L., Khonina, S.N. (2022). Environmental Monitoring: A Comprehensive Review on Optical Waveguide and Fiber-Based Sensors. *Biosensors* 12, 1038. https://doi.org/10.3390/bios12111038

Calderon, M., Reyes-Betanzo, C. (2023). Design and simulation of a piezoelectric micropump for drug delivery systems. *Microsyst. Technol.* 29, 253–264. https://doi.org/10.1007/s00542-023-05417-wChemistry. Hauptband, Fourteenth edition. ed, (2018). Pearson, New York.

Cheng, C.-H., Yang, A.-S., Cheng, H.-Y., Lai, M.-Y., (2015). Development of Piezoelectric Gas Micro Pumps with the PDMS Check Valve Design 9.

Ciuti, G., Ricotti, L., Menciassi, A., Dario, P., (2015). MEMS Sensor Technologies for Human Centred Applications in Healthcare, Physical Activities, Safety and Environmental Sensing: A Review on Research Activities in Italy. *Sensors* 15, 6441–6468. https://doi.org/10.3390/s150306441

Dinh, T.X., Dau, V.T., Sugiyama, S., Pham, P.H. (2010). Fluidic device with pumping and sensing functions for precise flow control. *Sens. Actuators B Chem*. 150, 819–824. https://doi.org/10.1016/j.snb.2010.08.009

Gidde, R.R., Pawar, P.M., Dhamgaye, V.P. (2020). Fully coupled modeling and design of a piezoelectric actuation based valveless micropump for drug delivery application. *Microsyst. Technol*. 26, 633–645. https://doi.org/10.1007/s00542-019-04535-8

Kaçar, A., Özer, M.B., Taşcıoğlu, Y., (2020). A Novel Artificial Pancreas: Energy Efficient Valveless Piezoelectric Actuated Closed-Loop Insulin Pump for T1DM. *Appl. Sci*. 10, 5294. https://doi.org/10.3390/app10155294

Labdelli, N., Soulimane, S., (2020). Conception of a New Generation of 3d Biomimetic Microvalves for Medical Application. *J. Serbian Soc. Comput. Mech*. 14, 99–112. https://doi.org/10.24874/jsscm.2020.14.01.09

Li, H., Liu, J., Li, K., Liu, Y., (2021). A review of recent studies on piezoelectric pumps and their applications. *Mech. Syst. Signal Process.* 151, 107393. https://doi.org/10.1016/j.ymssp.2020.107393

Liu, G., Yang, Z., Liu, J., Li, X., Wang, H., Zhao, T., Yang, X., (2014). A low cost, high performance insulin delivery system based on PZT actuation. Microsyst. Technol. 20, 2287–2294. https://doi.org/10.1007/s00542-014-2090-2

Munas, F., Melroy, G., Abeynayake, C., Chathuranga, H., Amarasinghe, R., Kumarage, P., Dau, V., Dao, D. (2018). Development of PZT Actuated Valveless Micropump. *Sensors* 18, 1302. https://doi.org/10.3390/s18051302

Nafea, M., Ali, M.S.M., Rehman, T., Mehranzamir, K. (2019). Geometrical Analysis of Diffuser-Nozzle Elements for Valveless Micropumps, in: 2019 *IEEE International Conference on Smart Instrumentation, Measurement and Application (ICSIMA*). Presented at the 2019 IEEE International Conference on Smart Instrumentation, Measurement and Application (ICSIMA), IEEE, Kuala Lumpur, Malaysia, pp. 1–5. https://doi.org/10.1109/ICSIMA47653.2019.9057345

Ni, J., Xuan, W., Li, Y., Chen, J., Li, W., Cao, Z., Dong, S., Jin, H., Sun, L., Luo, J. (2023). Analytical and experimental study of a valveless piezoelectric micropump with high flowrate and pressure load. Microsyst. *Nanoeng.* 9, 72. https://doi.org/10.1038/s41378-023-00547-7

Rusli, M., Chee, P.S., Arsat, R., Lau, K.X., Leow, P.L. (2018). Electromagnetic actuation dual-chamber bidirectional flow micropump. S*ens. Actuators Phys*. 282, 17–27. https://doi.org/10.1016/j.sna.2018.08.047

Schabmueller, C.G.J., Koch, M., Mokhtari, M.E., Evans, A.G.R., Brunnschweiler, A., Sehr, H., (2002). Self-aligning gas/liquid micropump. *J. Micromechanics Microengineering* 12, 420–424. https://doi.org/10.1088/0960-1317/12/4/313

Singh, S., Kumar, N., George, D., Sen, A.K., (2015). Analytical modeling, simulations and experimental studies of a PZT actuated planar valveless PDMS micropump. *Sens. Actuators Phys*. 225, 81–94. https://doi.org/10.1016/j.sna.2015.02.012

Slami, A., Soulimane, S. (2022). A Superimposed Valveless Micropump Using New Channels for Optimal Drug Delivery. *J. Serbian Soc. Comput. Mech*. 16, 45–53. https://doi.org/10.24874/jsscm.2022.16.01.04

Sta Apolónia, Bragança, Portugal, andrews.va.souza@alunos.ipb.pt, Victor, A., Ribeiro, J., Campus Sta Apolónia;Bragança;Portugal; jribeiro@ipb.pt, F. Araújo, F., CEFET/RJ Campus Angra dos Reis;Rio de Janeiro;Brasil; fernando.araujo@cefet-rj.br (2019). Study of PDMS characterization and its applications in biomedicine: A review. J. Mech. Eng. Biomech. 4, 1–9. https://doi.org/10.24243/JMEB/4.1.163

Stemme, E., Stemme, G. (1993). A valveless diffuser/nozzle-based fluid pump. Sens. Actuators Phys. 39, 159–167. https://doi.org/10.1016/0924-4247(93)80213-Z

Uhlig, S., Gaudet, M., Langa, S., Schimmanz, K., Conrad, H., Kaiser, B., Schenk, H. (2018). Electrostatically Driven In-Plane Silicon Micropump for Modular Configuration. *Micromachines* 9, 190. https://doi.org/10.3390/mi9040190

Wang, B., Chu, X., Li, E., Li, L. (2006). Simulations and analysis of a piezoelectric micropump. *Ultrasonics* 44, e643–e646. https://doi.org/10.1016/j.ultras.2006.05.018

Wang, J., Liu, Y., Shen, Y., Chen, S., Yang, Z. (2016). A Resonant Piezoelectric Diaphragm Pump Transferring Gas with Compact Structure. *Micromachines* 7, 219. https://doi.org/10.3390/mi7120219